Bose-Fermi duality in a quantum Otto heat engine with trapped repulsive bosons

Jinfu Chen,[1,2] Hui Dong,[2,*] and Chang-Pu Sun[1,2,†]

[1]*Beijing Computational Science Research Center, Beijing 100193, China*
[2]*Graduate School of China Academy of Engineering Physics, Haidian District, Beijing 100193, China*

Quantum heat engine with ideal gas has been well studied, yet the role of interaction was seldom explored. We construct a quantum Otto heat engine with N repulsive bosons in a one-dimensional (1D) hard wall box. With the advantage of exact solution using the Bethe ansatz, we obtain not only the exact numerical result of efficiency in all interacting strength c but also analytical results for strong interaction. We find the efficiency η approaches to the one of noninteracting case $\eta_{\text{non}} = 1 - (L_1/L_2)^2$ for strong interaction with the asymptotic behavior $\eta \sim \eta_{\text{non}} - 4(N-1)L_1(L_2 - L_1)/(cL_2^3)$. Here L_1 and L_2 are two trap sizes during the cycle. Such a phenomenon reflects the duality between 1D strongly repulsive bosons and free fermions. We observe and explain the appearance of a minimum efficiency at a particular interacting strength c and study its dependence on the temperature.

I. INTRODUCTION

In classical thermodynamics, piston model with ideal gas serves as a prototype to realize heat engines with different cycles, such as the Carnot and the Otto cycles [1,2]. The noninteracting gas makes it feasible to obtain very simple results for efficiency as well as other properties [1]. Such simplicity also enables direct extensions of similar discussions in quantum region to show unique features of quantum thermodynamics with single particles as well as few identical particles with or without interaction [3–10]. The difficulty arises when the interaction changes the energy spectrum in a complicated way for designing the quantum heat engine cycle. Recently, Bengtsson *et al.* explored the effect of the attractive interaction with exact numerical simulation and showed the increase of work output in the Szilard engine [11]. However, it remains unclear how the work conversion is affected by interactions in the widely used heat engine cycles, e.g., quantum Otto cycle.

In order to show the effect of internal interaction on the efficiency, we construct a quantum Otto heat engine with one-dimensional (1D) repulsive Bose gas in a hard wall box [12–14]. We concentrate on the effect of internal interaction of the working medium [15,16]. Quantum Otto cycle is a simple and feasible cycle in quantum thermodynamics [3,17] and has been studied extensively in many quantum systems [9,10,18–24]. The advantage of our model is its exact solution with the Bethe ansatz [12,25], which allows the analytical results to show the effect of interaction in quantum thermodynamics. We find that the efficiency of the heat engine first decreases, reaches to the minimum value, and, finally, approaches to the initial value along with the increasing of the interacting strength c. For strong interaction, the recovery of

*hdong@gscaep.ac.cn
†cpsun@csrc.ac.cn

the efficiency is explained by the Bose-Fermi duality [26,27]. We observe a dip for the efficiency with particular interacting strength. We also study how temperature affects the dip of the efficiency.

This paper is organized as follows. In Sec. II, we introduce the solution of a 1D interacting Bose gas in a hard wall box by the Bethe ansatz and build the quantum Otto heat engine on this model. In Sec. III, we give the asymptotic efficiency for large interacting strength and the numerical efficiency for any interacting strength. The Bose-Fermi duality is discussed on the efficiency of the Otto heat engine. We associate the efficiency with the ratios of the energy for different states and study the efficiency at different temperatures. The perturbation result for small interacting strength is calculated in the Appendix.

II. QUANTUM OTTO HEAT ENGINE WITH REPULSIVE BOSONS

In this section, we design the quantum Otto heat engine with 1D repulsive Bose gas in a hard wall box. The efficiency of the quantum Otto cycle for different interacting strength c is studied to explore the effect of the interaction on the quantum heat engine.

The Hamiltonian for N repulsive bosons in a 1D hard wall box is

$$H(L, c) = \sum_{i=1}^{N} \frac{p_i^2}{2m} + \frac{c}{m} \sum_{i<j} \delta(x_i - x_j) + V(\{x_i\}), \quad (1)$$

where p_i and x_i are the momentum and coordinate for ith particle with mass m. The interacting strength c is positive for repulsive interaction. The trap potential $V(\{x_i\})$ is the infinite square potential

$$V(\{x_i\}) = \begin{cases} 0 & \forall\, 0 \leqslant x_i \leqslant L \\ \infty & \exists\, x_i < 0, \text{ or } x_i > L \end{cases}. \quad (2)$$

Eigenstates can be obtained with the Bethe ansatz [12] for the current trap as $\psi_{\{k_i\}}(\{x_i\}) = \sum_P a(P) \exp(i \sum_{l=1}^{N} k_{P(l)} x_l)$, $0 \leqslant x_1 \leqslant x_2, \ldots, \leqslant x_N \leqslant L$, with the superposition coefficient $a(P)$. We are interested in the thermodynamic property and skip the concrete form of $a(P)$, whose explicit form can be found in Ref. [12]. The boundary condition gives the Bethe equation for the wave vectors as

$$k_i L = \pi n_i + \sum_{j \neq i} \left(\arctan \frac{c}{k_i - k_j} + \arctan \frac{c}{k_i + k_j} \right). \quad (3)$$

The eigenstate $|\{n_i\}\rangle$ is represented by a set of ordered number $1 \leqslant n_1 \leqslant n_2 \leqslant \cdots \leqslant n_N$, and the wave vectors satisfy $1 \leqslant k_1 \leqslant k_2 \leqslant \cdots \leqslant k_N$. The corresponding energy for the eigenstate $|\{n_i\}\rangle$ is

$$E_{\{n_i\}}^{(L,c)} = \frac{1}{2m} \sum_{i=1}^{N} k_i^2. \quad (4)$$

For noninteracting case $c = 0$, Eq. (3) becomes $k_i L = \pi n_i$, which gives the momentum for free bosons in the infinite square potential [2]. The total energy is $E_{\{n_i\}}^{(L,0)} = (\pi^2/2mL^2) \sum_{i=1}^{N} n_i^2$.

With given trap size L and interacting strength c, the density matrix for the system at the equilibrium state with temperature T is $\rho = \sum_{\{n_i\}} p_{\{n_i\}}(T, L, c) |\{n_i\}\rangle\langle\{n_i\}|$. The probability $p_{\{n_i\}}(T, L, c)$ on the eigenstate $|\{n_i\}\rangle$ is

$$p_{\{n_i\}}(T, L, c) = \frac{e^{-\frac{E_{\{n_i\}}^{(L,c)}}{k_B T}}}{Z(T, L, c)}, \quad (5)$$

with the partition function $Z(T, L, c) = \sum_{\{n_i\}} \exp[-E_{\{n_i\}}^{(L,c)}/kT]$. The internal energy of the system is $U(T, L, c) = \sum_{\{n_i\}} p_{\{n_i\}} E_{\{n_i\}}^{(L,c)}$.

Figure 1(a) shows the entropy-temperature (S-T) diagram for the classical Otto cycle. The current quantum Otto cycle consists four strokes similar to the classical Otto cycle, illustrated on the entropy-energy (S-$\langle H \rangle$) diagram in Fig. 1(b). Since the temperature of the state 1,3 may not be well defined, we include the S-$\langle H \rangle$ diagram for the quantum Otto heat engine, with $\langle H \rangle$ as the internal energy for a general state. Here the entropy is evaluated with the von Neumann entropy $S = -\text{Tr}[\rho \ln \rho]$ for all later discussions. The four strokes are specified as follows.

Stroke I ($1 \rightarrow 2$): Isochoric heating. Initially, the system does not necessarily stay at a thermal equilibrium state. The internal energy of the system at state 1 is $U_1 = \sum_{\{n_i\}} p_{\{n_i\}}^{(1)} E_{\{n_i\}}^{(L_1,c)}$. With the fixed trap size L_1, the system contacts with the hot reservoir and reaches the thermal equilibrium state with temperature T_2. The internal energy at state 2 is $U_2 = \sum_{\{n_i\}} p_{\{n_i\}}^{(2)} E_{\{n_i\}}^{(L_1,c)}$ with the equilibrium occupation $p_{\{n_i\}}^{(2)} = p_{\{n_i\}}(T_2, L_1, c) = \exp[-\frac{E_{\{n_i\}}^{(L_1,c)}}{k_B T_2}]/Z(T_2, L_1, c)$. The internal energy increases by absorbing heat from the hot reservoir $Q_1 = U_2 - U_1 > 0$.

Stroke II ($2 \rightarrow 3$): Quantum adiabatic expansion. During the process, the system is isolated from any reservoir, and the trap size increases from L_1 to L_2 slowly in order to keep the occupation number unchanged, namely $p_{\{n_i\}}^{(3)} = p_{\{n_i\}}^{(2)}$. In this process, the internal energy decreases
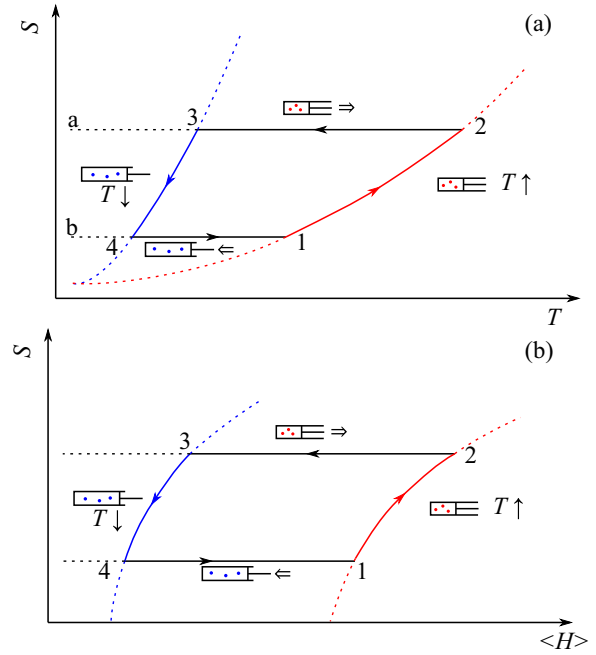

FIG. 1. (a) Entropy-temperature (S-T) diagram for the classical Otto heat engine. (b) Entropy-energy (S-$\langle H \rangle$) diagram for the quantum Otto heat engine. In both subfigures, the red (right) and blue (left) solid lines with arrows are isochoric processes contacting to the cold and hot reservoir with the corresponding trap size as L_1 and L_2, while the black (up and down) solid lines are adiabatic processes.

from $U_2 = \sum_{\{n_i\}} p_{\{n_i\}}^{(2)} E_{\{n_i\}}^{(L_1,c)}$ to $U_3 = \sum_{\{n_i\}} p_{\{n_i\}}^{(3)} E_{\{n_i\}}^{(L_2,c)}$ to export work $W_1 = U_3 - U_2 = \sum_{\{n_i\}} p_{\{n_i\}}^{(2)} [E_{\{n_i\}}^{(L_2,c)} - E_{\{n_i\}}^{(L_1,c)}] < 0$. After the expansion, the system usually reaches a nonequilibrium state, without well-defined temperature [3].

Stroke III ($3 \rightarrow 4$): Isochoric cooling. Similarly to stroke I, the trap size is fixed at L_2. The system contacts with the cold reservoir and reaches the thermal equilibrium state with temperature T_4. The occupation is $p_{\{n_i\}}^{(4)} = p_{\{n_i\}}(T_4, L_2, c) = \exp[-\frac{E_{\{n_i\}}^{(L_2,c)}}{k_B T_4}]/Z(T_4, L_2, c)$, and the internal energy is $U_4 = \sum_{\{n_i\}} p_{\{n_i\}}^{(4)} E_{\{n_i\}}^{(L_2,c)}$. The internal energy decreases by releasing heat to the cold reservoir $Q_2 = U_4 - U_3 < 0$.

Stroke IV ($4 \rightarrow 1$): Quantum adiabatic compressing. Similarly to stroke II, the system is isolated from any reservoir, and the trap size decreases from L_2 to L_1 slowly to keep the probability $p_{\{n_i\}}$ as a constant, namely $p_{\{n_i\}}^{(1)} = p_{\{n_i\}}^{(4)}$. The system reaches a nonequilibrium state as the initial state of stroke I. The internal energy increases by performed work $W_2 = U_1 - U_4 = \sum_{\{n_i\}} p_{\{n_i\}}^{(4)} [E_{\{n_i\}}^{(L_1,c)} - E_{\{n_i\}}^{(L_2,c)}] > 0$.

III. EFFICIENCY AND INTERACTION

For large interacting strength c, we have the expansion of Eq. (3) to the first order of $1/c$ as

$$k_i L = \pi(n_i + i - 1) - \sum_{j \neq i} \left(\frac{k_i - k_j}{c} + \frac{k_i + k_j}{c} \right), \quad (6)$$

where we have used the expansion $\arctan(x) = \frac{\pi}{2}\text{sgn}(x) - \frac{1}{x} + o(\frac{1}{x^2})$ for large x. The additional phase $(i-1)\pi$ in

Eq. (6) comes from the summation of j when $j < i$. Equation (6) gives the solution for the wave vector $k_i = \pi(n_i + i - 1)/(L + 2(N-1)/c)$. The asymptotic energy for the eigenstate $|\{n_i\}\rangle$ is

$$E_{\{n_i\}}^{(L,c)} = \frac{\pi^2}{2m} \frac{\sum_{i=1}^{N} (n_i + i - 1)^2}{\left[L + \frac{2(N-1)}{c}\right]^2}. \tag{7}$$

The energy ratios for eigenstates with different trap size have the same value,

$$\frac{E_{\{n_i\}}^{(L_2,c)}}{E_{\{n_i\}}^{(L_1,c)}} = \left[\frac{L_1 + \frac{2(N-1)}{c}}{L_2 + \frac{2(N-1)}{c}}\right]^2. \tag{8}$$

Therefore, the internal energy for the initial state and the final state of the quantum adiabatic processes has the same ratio as

$$\frac{U_3}{U_2} = \frac{U_4}{U_1} = \left[\frac{L_1 + \frac{2(N-1)}{c}}{L_2 + \frac{2(N-1)}{c}}\right]^2. \tag{9}$$

With the unchanged occupation number $p_{\{n_i\}}^{(3)} = p_{\{n_i\}}^{(2)}$ and $p_{\{n_i\}}^{(4)} = p_{\{n_i\}}^{(1)}$ in quantum adiabatic processes, the extracted work for the quantum Otto cycle is

$$W_{\text{out}} = -W_1 - W_2$$
$$= \sum_{\{n_i\}} \left[p_{\{n_i\}}^{(2)} - p_{\{n_i\}}^{(4)}\right]\left[E_{\{n_i\}}^{(L_1,c)} - E_{\{n_i\}}^{(L_2,c)}\right], \tag{10}$$

which should be positive to ensure a valid heat engine. For large interacting strength c, we derive the positive work condition by Eq. (8)

$$\frac{T_2}{T_4} > \left[\frac{L_2 + \frac{2(N-1)}{c}}{L_1 + \frac{2(N-1)}{c}}\right]^2. \tag{11}$$

The efficiency $\eta = W_{\text{out}}/Q_1$ is written explicitly as

$$\eta = \frac{\sum_{\{n_i\}} \left[p_{\{n_i\}}^{(2)} - p_{\{n_i\}}^{(4)}\right]\left[E_{\{n_i\}}^{(L_1,c)} - E_{\{n_i\}}^{(L_2,c)}\right]}{\sum_{\{n_i\}} \left[p_{\{n_i\}}^{(2)} - p_{\{n_i\}}^{(4)}\right]E_{\{n_i\}}^{(L_1,c)}}. \tag{12}$$

In the following numerical calculations, we use Eq. (12) to calculate the exact efficiency. At the strong interaction limit, we obtain the efficiency as

$$\eta = 1 - \left[\frac{L_1 + \frac{2(N-1)}{c}}{L_2 + \frac{2(N-1)}{c}}\right]^2$$
$$\approx \eta_{\text{non}} - \frac{4L_1(L_2 - L_1)}{L_2^3} \frac{(N-1)}{c}. \tag{13}$$

Such efficiency approaches the one of noninteracting bosons or fermions $\eta_{\text{non}} = 1 - L_1^2/L_2^2$, the same for the single-particle quantum Otto heat engine [3]. The first order of the deviation is $\sim N/c$, proportional to the particle number or the particle density in the box. The recovery of the efficiency at strong coupling limit is caused by the duality between fermions and interacting bosons in the 1D case [12,27]. Such duality shows the match between energy levels of strong repulsive interacting bosons and noninteracting fermions or vice versa. We show this duality on the efficiency of the quantum Otto heat engine.
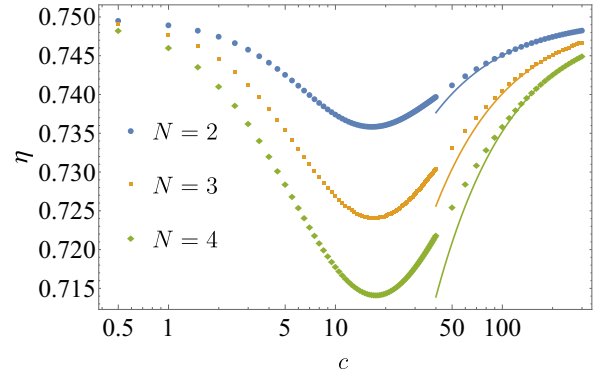

FIG. 2. Log-linear plot for the efficiency η for the quantum Otto heat engine with different interacting strength c. We consider three cases with the particle number as $N = 2, 3, 4$, and choose the temperature as $T_2 = 50$, $T_4 = 8$. For all numerical calculations, the mass and the cutoff of the quantum number are set as $m = 1$ and $n_{\text{cut}} = 20$, and the trap size is always set as $L_1 = 1$, $L_2 = 2$. The solid line is the analytical result of the asymptotic efficiency for large c by Eq. (13), while the dots are the exact numerical result.

For small interacting strength c, we have calculated the efficiency for two interacting bosons in perturbation. The energy $E_{n_1,n_2}^{(L,c)}$ to the first order of the interacting strength c is

$$E_{n_1,n_2}^{(L,c)} = \frac{1}{2m}\frac{\pi^2(n_1^2 + n_2^2)}{L^2} + \left(2 - \frac{1}{2}\delta_{n_1,n_2}\right)\frac{c}{mL} + o(c). \tag{14}$$

We keep all terms in Eq. (12) to the first order of the interacting strength c. The efficiency is obtained as

$$\eta = \eta_{\text{non}} + \frac{1}{2}\frac{L_2 - L_1}{L_2^2}\frac{\sum_n \delta p_{n,n}^{c=0}}{\sum_{n_1,n_2}\delta p_{n_1,n_2}^{c=0}E_{n_1,n_2}^{(L_1,0)}}\frac{c}{m} + o(c), \tag{15}$$

where $\delta p_{n_1,n_2}^{c=0} = p_{n_1,n_2}^{(2)} - p_{n_1,n_2}^{(4)}$ is the difference of two equilibrium occupations of the state (n_1, n_2) for two free bosons. The derivation of Eqs. (14) and (15) is attached in the Appendix. We compare the efficiency derived by Eq. (15) and the exact numerical result in Fig. 5 under weak interaction limit in the Appendix, which shows the perturbation works well when $cL_1 < 0.1$.

To validate our result in Eq. (13), we compare it to the exact numerical result in Fig. 2. The efficiency for heat engine with different numbers $N = 2, 3, 4$ of bosons are plotted as functions of interacting strength c. For the exact numerical calculation, we set the mass and the Boltzmann constant as $m = 1$, $k_B = 1$, and choose a cutoff $n_{\text{cut}} = 20$ for the energy level index n_i, namely $n_i \leqslant n_{\text{cut}}$. We have verified that the cutoff is large enough to obtain convergent result for the temperature we have considered $T \leqslant 250$. We calculate the energy levels $E_{\{n_i\}}^{(L_1,c)}$ and $E_{\{n_i\}}^{(L_2,c)}$ by exactly solving Eq. (3) with the trap size as $L_1 = 1$ and $L_2 = 2$ and obtain the probability $p_{\{n_i\}}^{(2)}$ and $p_{\{n_i\}}^{(4)}$ for the equilibrium states 2 and 4 with the temperature $T_2 = 50$ and $T_4 = 8$ for the hot and cold reservoirs, respectively. The exact efficiency is evaluated via Eq. (12) with the probability $p_{\{n_i\}}^{(j)}$, $j = 2, 4$ and the energy levels $E_{\{n_i\}}^{(L_j,c)}$, $j = 1, 2$. Figure 2 shows that the numerical
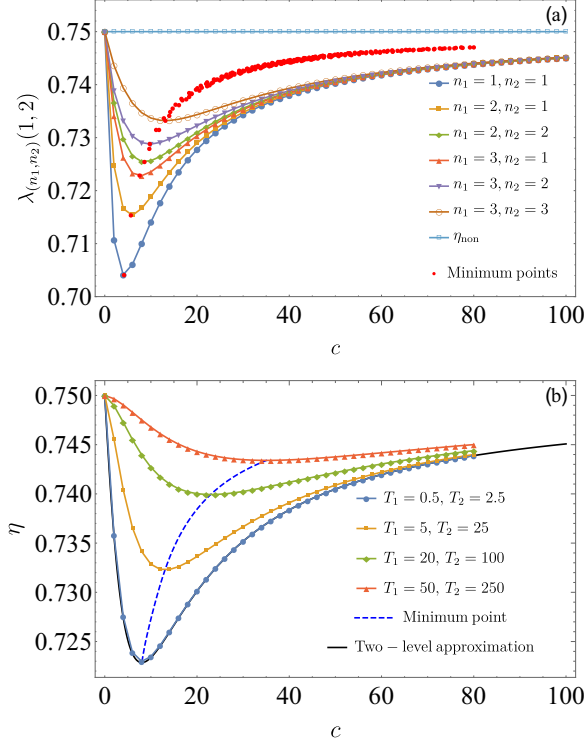
FIG. 3. (a) The ratio of the energy $\lambda_{\{n_i\}}(L_1, L_2) = 1 - E_{\{n_i\}}^{(L_2,c)}/E_{\{n_i\}}^{(L_1,c)}$ with different interacting strength c for two interacting bosons $N = 2$. We show the ratio for the state with the quantum number $(n_1, n_2) = (1, 1), (1, 2), (1, 3), (2, 2), (2, 3), (3, 3)$. The solid lines with different markers are the ratios for six corresponding energy levels and the efficiency of noninteracting case $\eta_{\text{non}} = 1 - L_1^2/L_2^2 = 0.75$. The red dots are the minimum point of the ratio, including energy levels not plotted. (b) The efficiency for different temperature T_1 and T_2 and two-state approximation result. The solid lines with different markers are the exact numerical result for different temperature T_1 and T_2, where the blue dashed line shows the the minimum point of the efficiency. The black solid line is derived by the two-level approximation from Eq. (17). The result of two-level approximation matches well with the one at low-temperature limit $T_4 = 0.5$, $T_2 = 2.5$.

result matches the analytical result by Eq. (13) well for the large interacting strength.

Interestingly, the curve for efficiency shows a dip with particular interacting strength c in Fig. 2. To understand the appearance of such dip, we rewrite the efficiency in Eq. (12) as

$$\eta = \frac{\sum_{\{n_i\}} \left[p_{\{n_i\}}^{(2)} - p_{\{n_i\}}^{(4)} \right] E_{\{n_i\}}^{(L_1,c)} \lambda_{\{n_i\}}(L_1, L_2)}{\sum_{\{n_i\}} \left[p_{\{n_i\}}^{(2)} - p_{\{n_i\}}^{(4)} \right] E_{\{n_i\}}^{(L_1,c)}}, \quad (16)$$

where $\lambda_{\{n_i\}}(L_1, L_2) = 1 - E_{\{n_i\}}^{(L_2,c)}/E_{\{n_i\}}^{(L_1,c)}$ is a ratio of the energy, similar to the Otto efficiency for a two-level heat engine [3]. In Fig. 3(a), we plot the ratio $\lambda_{\{n_i\}}(L_1, L_2)$ as a function of the interacting strength c for different energy levels $\{n_i\}$. The curves for different energy levels show dips with different positions. For low temperature, since the particle occupation on higher energy levels can be neglected, we use a two-level approximation to calculate the efficiency,
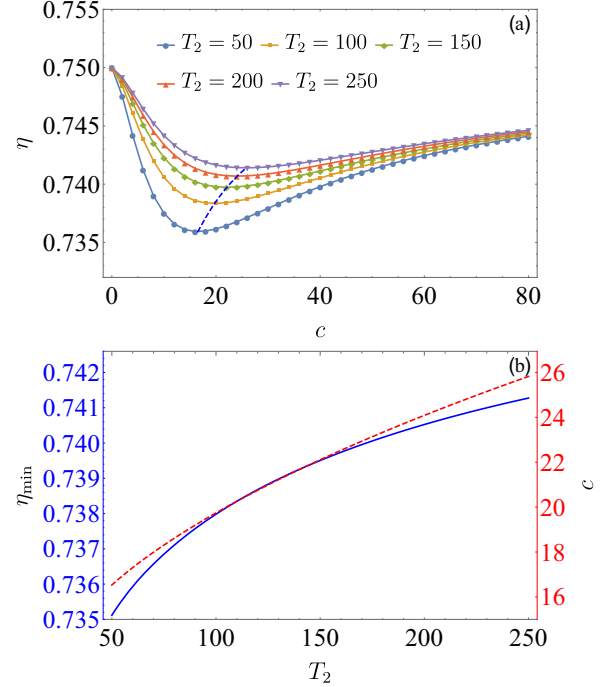
$$\eta = 1 - \frac{\Delta_2}{\Delta_1}, \quad (17)$$

FIG. 4. (a) Efficiency-interaction curve with different temperature of the hot reservoir T_2. The temperature of the hot reservoir T_2 changes from 50 to 250, while the temperature of the cold reservoir is fixed at $T_4 = 8$. The solid lines with different markers represent the efficiency η for different temperature T_2. The blue dashed line shows the the minimum point of the efficiency for different temperature T_2. (b) Minimum-efficiency point with different T_2. We extract the coordinate of the minimum point for different T_2 in Fig. 4(a). The blue solid line and the red dashed line give the minimum efficiency η_{min} and the interacting strength c for the the minimum point for different T_2 respectively.

where only the ground state and the first excited state are considered with the energy gap $\Delta_i = E_{(2,1)}^{(L_i,c)} - E_{(1,1)}^{(L_i,c)}$, $i = 1, 2$. Figure 3(b) shows that the efficiency derived with two-level approximation matches with the exact numerical result at low-temperature limit $T_2 = 2.5$, $T_4 = 0.5$. For high temperature, the efficiency contains more of a contribution from high energy levels, and the efficiency approaches the noninteracting case η_{non}.

The efficiency of this Otto heat engine is affected by the temperature of the reservoirs. This property is different from the single-particle quantum Otto heat engine [3]. In Fig. 4, we study the temperature effect by modulating the temperature of the hot reservoir T_2 from 50 to 250 with the fixed temperature of the cold reservoir at $T_4 = 8$. Figure 4(a) shows that the efficiency η is larger for higher temperature T_2 as expected. The minimum point of the efficiency for different temperature T_2 is plotted with blue dashed line. To figure out how the temperature T_2 affects the minimum point of the efficiency, we plot both the efficiency η_{min} and the interacting strength c of the minimum point with different temperature T_2 in Fig. 4(b). The interacting strength c (the red dashed line) and the efficiency η_{min} (the blue solid line) for the minimum efficiency become larger when T_2 increases, which matches the minimum point of $\lambda_{\{n_i\}}(L_1, L_2)$ in Fig. 3. The behavior of

the efficiency with different temperature T_2 matches with the change of $\lambda_{\{n_i\}}(L_1, L_2)$ of the corresponding energy levels.

IV. CONCLUSION

We have studied the quantum Otto heat engine with 1D repulsive Bose gas in a hard wall box to reveal the effect of interaction on the efficiency. For weak interaction, we conclude that the efficiency of the Otto heat engine is lower than the noninteracting case. For strong interaction, the efficiency approaches to its initial value, which is explained by the Bose-Fermi duality for 1D interacting Bose gas. With a given interacting strength, the efficiency decreases when the temperature of the reservoirs is lower. By calculating the ratio of the energy $\lambda_{\{n_i\}}(L_1, L_2)$, we have explained the appearance of the minimum value of efficiency as the function of the interacting strength c. For the low-temperature case, the two-level approximation gives a good result with different interacting strength. For the high-temperature case, the contribution for high energy levels shifts the minimum position of the efficiency.

ACKNOWLEDGMENTS

APPENDIX: WEAK INTERACTION LIMIT

In this Appendix, we derive the result in the weak interaction limit for two interacting bosons. We expand Eq. (3) to the first order of c and obtain the equations for k_1 and k_2,

$$
(k_1 + k_2)L = \pi(n_1 + n_2) + 2\frac{c}{k_1 + k_2} + o(c)
$$
$$
(k_1 - k_2)L = \pi(n_1 - n_2) + 2\frac{c}{k_1 - k_2} + o(c). \tag{A1}
$$

For $n_1 \neq n_2$, the solutions for k_1 and k_2 to the first order of c are

$$
k_1 = \frac{\pi}{L}n_1 + 2\frac{c}{\pi}\frac{n_1}{n_1^2 - n_2^2} + o(c)
$$
$$
k_2 = \frac{\pi}{L}n_2 - 2\frac{c}{\pi}\frac{n_2}{n_1^2 - n_2^2} + o(c). \tag{A2}
$$

The corresponding energy is

$$
E_{n_1,n_2}^{(L,c)} = \frac{\pi^2}{2mL^2}(n_1^2 + n_2^2) + 2\frac{c}{mL} + o(c). \tag{A3}
$$

For $n_1 = n_2$, the solution is

$$
k_1 = \frac{\pi}{L}n_1 + \frac{c}{2\pi n_1} + \sqrt{\frac{c}{2L}} + o(c)
$$
$$
k_2 = \frac{\pi}{L}n_1 + \frac{c}{2\pi n_1} - \sqrt{\frac{c}{2L}} + o(c). \tag{A4}
$$

The corresponding energy is

$$
E_{n_1,n_2}^{(L,c)} = \frac{\pi^2}{mL^2}n_1^2 + \frac{3c}{2mL} + o(c). \tag{A5}
$$

The general result of the energy is

$$
E_{n_1,n_2}^{(L,c)} = \frac{1}{2m}\frac{\pi^2(n_1^2 + n_2^2)}{L^2} + \left(2 - \frac{1}{2}\delta_{n_1,n_2}\right)\frac{c}{mL} + o(c). \tag{A6}
$$

From the expansion of the exponential

$$
e^{-\frac{E_{\{n_i\}}^{(L_1,c)}}{k_B T_2}} = e^{-\frac{\frac{1}{2m}\frac{\pi^2(n_1^2 + n_2^2)}{L^2}}{k_B T_2}}\left[1 - \frac{\left(2 - \frac{1}{2}\delta_{n_1,n_2}\right)\frac{c}{mL}}{k_B T_2}\right] + o(c), \tag{A7}
$$

we calculate the expansion for the probability as

$$
p_{n_1,n_2}(T, L, c)
$$
$$
= p_{n_1,n_2}(T, L, 0)\left\{1 + \frac{\frac{1}{2}\left[\delta_{n_1,n_2} - \sum_j p_{j,j}(T, L, 0)\right]}{k_B T_2}\frac{c}{mL}\right\}
$$
$$
+ o(c). \tag{A8}
$$

The difference of the population in Eq. (12) is expanded to the first order of the interacting strength

$$
p_{\{n_i\}}^{(2)} - p_{\{n_i\}}^{(4)} = \delta p_{n_1,n_2}^{c=0} + \Theta_{n_1,n_2}c + o(c), \tag{A9}
$$

with

$$
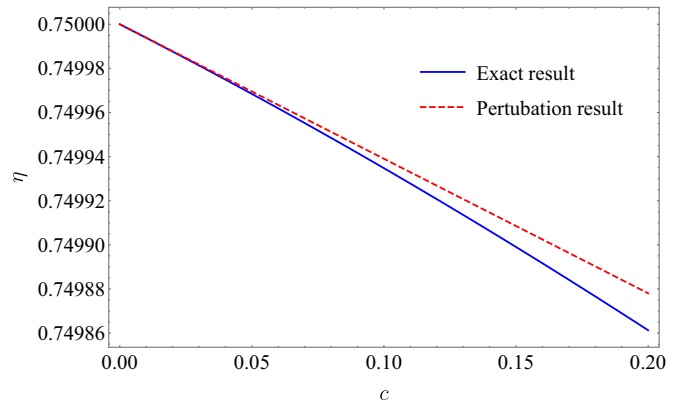\delta p_{n_1,n_2}^{c=0} = p_{n_1,n_2}(T_2, L_1, 0) - p_{n_1,n_2}(T_4, L_2, 0) \tag{A10}
$$

FIG. 5. The efficiency of quantum Otto heat engine with two interacting bosons for small c. The parameters are same as Fig. 2. The red dashed line is obtained by Eq. (15), while the blue solid line is exact result solved by the Bethe equation.

and

$$\Theta_{n_1,n_2} = \frac{1}{2} \left\{ p_{n_1,n_2}(T_2, L_1, 0) \frac{\left[\delta_{n_1,n_2} - \sum_j p_{j,j}(T_2, L_1, 0) \right]}{k_B T_2 m L_1} \right.$$

$$\left. - p_{n_1,n_2}(T_4, L_2, 0) \frac{\left[\delta_{n_1,n_2} - \sum_j p_{j,j}(T_4, L_2, 0) \right]}{k_B T_4 m L_2} \right\}.$$

(A11)

$\delta p_{n_1,n_2}^{c=0}$ and Θ_{n_1,n_2} are independent on the interacting strength c. Finally, we obtain the efficiency for weak interaction as

$$\eta = 1 - \frac{L_1^2}{L_2^2} + \frac{1}{2} \frac{L_2 - L_1}{L_2^2} \frac{\sum_n \delta p_{n,n}^{c=0}}{\sum_{n_1,n_2} \delta p_{n_1,n_2}^{c=0} E_{n_1,n_2}^{(L_1,0)}} \frac{c}{m} + o(c).$$

(A12)

Figure 5 shows the perturbation result by Eq. (A12) and the exact numerical result under weak interaction limit. The slope is verified to be negative $\sum_n \delta p_{n,n}^{c=0} / \sum_{n_1,n_2} \delta p_{n_1,n_2}^{c=0} E_{n_1,n_2}^{(L_1,0)} < 0$. The perturbation result shows that the efficiency linearly decreases for small c.

---

[1] H. B. Callen, *Thermodynamics and an Introduction to Thermostatistics*, 2nd ed. (Wiley, New York, 1985).

[2] K. Huang, *Statistical Mechanics*, 2nd ed. (Wiley, New York, 1987).

[3] H. T. Quan, Y. X. Liu, C. P. Sun, and F. Nori, Phys. Rev. E **76**, 031105 (2007).

[4] H. Dong, D. Z. Xu, C. Y. Cai, and C. P. Sun, Phys. Rev. E **83**, 061108 (2011).

[5] S. W. Kim, T. Sagawa, S. DeLiberato, and M. Ueda, Phys. Rev. Lett. **106**, 070401 (2011).

[6] C. Y. Cai, H. Dong, and C. P. Sun, Phys. Rev. E **85**, 031114 (2012).

[7] D. Gelbwaser-Klimovsky, W. Niedenzu, and G. Kurizki, in *Advances in Atomic, Molecular, and Optical Physics* (Elsevier, Amsterdam, 2015), pp. 329–407.

[8] H. T. Quan, Phys. Rev. E **79**, 041129 (2009).

[9] J. Jaramillo, M. Beau, and A. del Campo, New J. Phys. **18**, 075019 (2016).

[10] M. Beau, J. Jaramillo, and A. del Campo, Entropy **18**, 168 (2016).

[11] J. Bengtsson, M. N. Tengstrand, A. Wacker, P. Samuelsson, M. Ueda, H. Linke, and S. M. Reimann, Phys. Rev. Lett. **120**, 100601 (2018).

[12] M. Gaudin, Phys. Rev. A **4**, 386 (1971).

[13] M. T. Batchelor, X. W. Guan, N. Oelkers, and C. Lee, J. Phys. A: Math. Gen. **38**, 7787 (2005).

[14] N. Oelkers, M. T. Batchelor, M. Bortz, and X.-W. Guan, J. Phys. A: Math. Gen. **39**, 1073 (2006).

[15] Y.-H. Ma, S.-H. Su, and C.-P. Sun, Phys. Rev. E **96**, 022143 (2017).

[16] S. Çakmak, F. Altintas, and Özgür E. Müstecaplıoğlu, Eur. Phys. J. Plus **131**, 1 (2016).

[17] D. Newman, F. Mintert, and A. Nazir, Phys. Rev. E **95**, 032139 (2017).

[18] G. Thomas and R. S. Johal, Phys. Rev. E **83**, 031135 (2011).

[19] W. Hübner, G. Lefkidis, C. D. Dong, D. Chaudhuri, L. Chotorlishvili, and J. Berakdar, Phys. Rev. B **90**, 024401 (2014).

[20] F. Altintas, A. U. C. Hardal, and Özgür E. Müstecaplıoğlu, Phys. Rev. E **90**, 032102 (2014).

[21] K. Zhang, F. Bariani, and P. Meystre, Phys. Rev. Lett. **112**, 150602 (2014).

[22] E. A. Ivanchenko, Phys. Rev. E **92**, 032124 (2015).

[23] S. Deng, A. Chenu, P. Diao, F. Li, S. Yu, I. Coulamy, A. del Campo, and H. Wu, Sci. Adv. **4**, eaar5909 (2018).

[24] X. Huang, Q. Sun, D. Guo, and Q. Yu, Physica A **491**, 604 (2018).

[25] C. N. Yang, Phys. Rev. Lett. **19**, 1312 (1967).

[26] M. Girardeau, J. Math. Phys. **1**, 516 (1960).

[27] B. Wang, J. Zhang, and H. T. Quan, Phys. Rev. E **97**, 052136 (2018).